Superconductivity and quantum criticality in the heavy-fermion system β-$YbAlB_4$

S. NAKATSUJI[1]*, K. KUGA[1,2], Y. MACHIDA[1], T. TAYAMA[1], T. SAKAKIBARA[1], Y. KARAKI[1], H. ISHIMOTO[1], S. YONEZAWA[2], Y. MAENO[2], E. PEARSON[3], G. G. LONZARICH[3], L. BALICAS[4], H. LEE[4†] AND Z. FISK[5]

[1]Institute for Solid State Physics (ISSP), University of Tokyo, Kashiwa 277-8581, Japan
[2]Department of Physics, Kyoto University, Kyoto 606-8502, Japan
[3]Cavendish Laboratory, Madingley Road, Cambridge CB3 OHE, UK
[4]National High Magnetic Field Laboratory (NHMFL), Tallahassee, Florida 32310, USA
[5]Department of Physics and Astronomy, University of California, Irvine, California 92697, USA
[†]Present address: Los Alamos National Laboratory, Los Alamos, New Mexico 87545, USA
*e-mail: satoru@issp.u-tokyo.ac.jp

Published online: 29 June 2008; corrected online: 11 July 2008; doi:10.1038/nphys1002

A long-standing question in the field of superconductivity is whether pairing of electrons can arise in some cases as a result of magnetic interactions instead of electron–phonon-induced interactions as in the conventional Bardeen–Cooper–Schrieffer theory[1]. A major challenge to the idea of magnetically mediated superconductivity has been the dramatically different behaviour of the cerium and ytterbium heavy-fermion compounds. The cerium-based systems are often found to be superconducting[1–6], in keeping with a magnetic pairing scenario, but corresponding ytterbium systems, or hole analogues of the cerium systems, are not. Despite searches over two decades there has been no evidence of heavy-fermion superconductivity in an ytterbium system, casting doubt on our understanding of the electron–hole parallelism between the cerium and the ytterbium compounds. Here we present the first empirical evidence that superconductivity is indeed possible in an ytterbium-based heavy-fermion system. In particular, we observe a superconducting transition at $T_c = 80$ mK in high-purity single crystals of $YbAlB_4$ in the new structural β phase[7]. We also observe a novel type of non-Fermi-liquid state above T_c that arises without chemical doping, in zero applied magnetic field and at ambient pressure, establishing β-$YbAlB_4$ as a unique system showing quantum criticality without external tuning.

First we present the bulk magnetic and electronic properties of β-$YbAlB_4$, a new morphology of the previously known α-$YbAlB_4$ (refs 7,8). Shown in Fig. 1a is the orthorhombic crystal structure of β-$YbAlB_4$ and the temperature dependence of the d.c. magnetic susceptibility $\chi = M/H$. Here, M and H represent the magnetization and external field, respectively. The magnetic susceptibility shows the strong uniaxial anisotropy of an Ising system with moments aligned along the c axis. Above 100 K the c-axis susceptibility has a Curie–Weiss form $\chi_c(T) = C/(T - \theta_W)$, with $\theta_W \sim -210$ K and a Curie constant C corresponding to an effective Ising moment $\mu_{eff} = g_J J_Z \sim 3.1\,\mu_B$, where g_J is the Landé g factor and J_Z is the c-axis component of the total angular momentum. The in-plane susceptibility, on the other hand, is almost temperature independent, showing a weak peak around 200 K.

Shown in Fig. 1b is the temperature dependence of the in-plane resistivity, ρ_{ab}, along with the estimated $4f$-electron contribution ρ_m (defined in the figure caption), which shows a coherence peak at about 250 K. The low residual resistivity $\rho_{ab}(0) \sim 0.4\,\mu\Omega$ cm and correspondingly high residual resistivity ratio, $\rho_{ab}(300\,\mathrm{K})/\rho_{ab}(0) \sim 300$, suggest that the electronic mean free path is of the order of 0.1 μm.

In contrast to most other heavy-fermion compounds, the resistivity does not show a Fermi liquid (FL) regime characterized by a T^2 temperature variation (Fig. 1b). As shown in Fig. 1b insets, ρ_{ab} is linear between 4 and 1 K and varies as $T^{1.5}$ below $T_0 \sim 1$ K down to 80 mK. Below 80 mK our highest-purity samples are superconducting (Fig. 1b, insets). We shall return to this key finding presently.

The effect of an applied magnetic field on the temperature dependence of the in-plane resistivity is shown in Fig. 2. It is seen that the FL form of ρ_{ab} is rapidly restored in a magnetic field (blue region in Fig. 2b) and that the non-FL form discussed above with a temperature exponent of 1.5 (yellow region) exists only below about 0.1 T.

As shown in Fig. 3a,b, non-FL behaviour is also seen in the susceptibility χ_c and the magnetic part of the specific heat C_M (defined in the figure caption). In zero magnetic field $\chi_c \sim T^{-1/3}$ and $C_M/T \sim (S^*/T^*)\ln(T^*/T)$ up to crossover temperatures T_0 of the order of 2 K and 3 K, respectively. The values of T_0 for the resistivity, susceptibility and specific heat are thus similar. A fit to the specific-heat data gives $S^* \sim 5.1\,\mathrm{J/(mol\,Yb\,K)}$, a value close to $R\ln 2$. $T^* \sim 200\,\mathrm{K} \sim \theta_W$ may be interpreted as the temperature at which the entropy of a ground state doublet is recovered.

As in the cases of ρ_{ab}, we find that an applied field rapidly restores FL behaviour, that is, both χ_c and C_M/T saturate at low T. C_M/T saturates at above $150\,\mathrm{mJ/(mol\,Yb\,K^2)}$, a value consistent with that expected for a heavy-fermion system.

The FL state can be characterized by the low-T limits of $A = (\rho_{ab}(T) - \rho_{ab}(0))/T^2$, χ_c and $\gamma = C_M/T$. In the following the saturation values of χ_c and C_M/T are taken at 80 mK and 400 mK, respectively. From Fig. 3c we see that in order of magnitude our data roughly agree with the relations $A \propto \gamma^2 \propto \chi^2$, so $\gamma \propto \chi$ in the FL regime between 0.5 and 4 T. The ratio A/γ^2, the Kadowaki–Woods ratio, is of order $3 \times 10^{-5}\,\mu\Omega\,\mathrm{cm\,K^{-2}(mol\,K^2\,mJ^{-1})^2}$ and similar to that found in other heavy-fermion compounds[9]. The ratio χ/γ gives a Wilson ratio, $R_W = \pi^2 k_B^2/(\mu_0 \mu_{eff}^2)(\chi/\gamma)$, of the order of

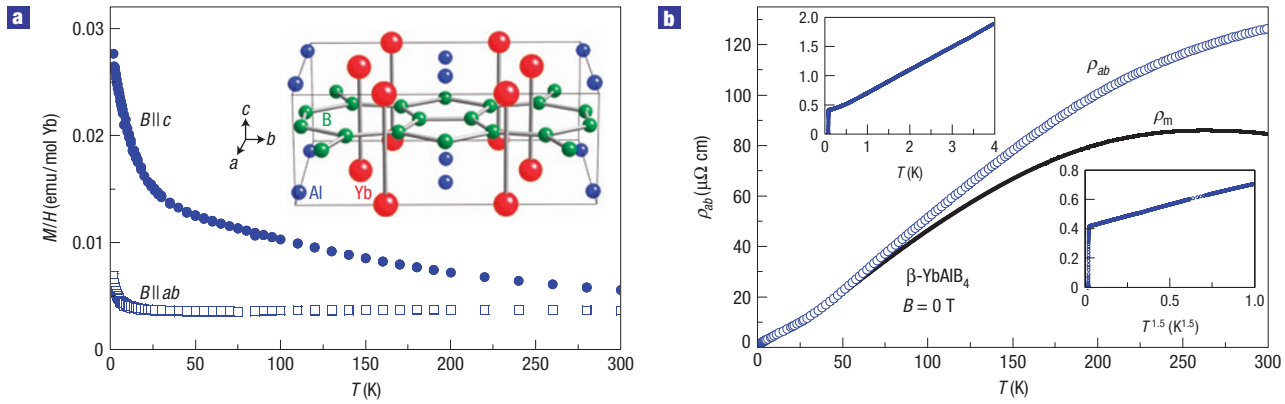

Figure 1 Physical properties of β-YbAlB$_4$. a, Temperature dependence of the d.c. susceptibility M/H measured in a field of 100 mT along the ab plane and c axis. The c-axis susceptibility changes in slope around 40 K. This is most likely due to a crystal-electric-field splitting Δ, separating the ground-state Kramers doublet and the excited states. Inset, the crystallographic unit cell of β-YbAlB$_4$. It has an orthorhombic (*Cmmm*) space group with lattice parameters $a = 0.73080(4)$ nm, $b = 0.93150(5)$ nm, $c = 0.34980(2)$ nm and can be viewed as an interleaving of planar B nets and Yb/Al layers[7]. Interestingly, the closest Yb–Yb contact is 0.34980(2) nm, corresponding to c, which is slightly more than twice the metallic radius of Yb^{3+} (0.174 nm). The underlying structural unit for magnetism may well be a one-dimensional chain of Yb^{3+} penetrating the B net. **b**, Temperature dependence of zero-field in-plane resistivity ρ_{ab} (open circle) and its 4f-electron contribution ρ_m (solid line). The latter was estimated by subtracting the temperature dependence of ρ_{ab} for β-LuAlB$_4$, the non-magnetic isostructural analogue of β-YbAlB$_4$ (ref. 7). No superconductivity is found for β-LuAlB$_4$ down to $T = 35$ mK. A slight change in slope of ρ_m around 40 K is attributable to a crystal-electric-field effect. Insets, Low-temperature part of $\rho_{ab}(T)$ versus T (top left) and $T^{1.5}$ (bottom right).

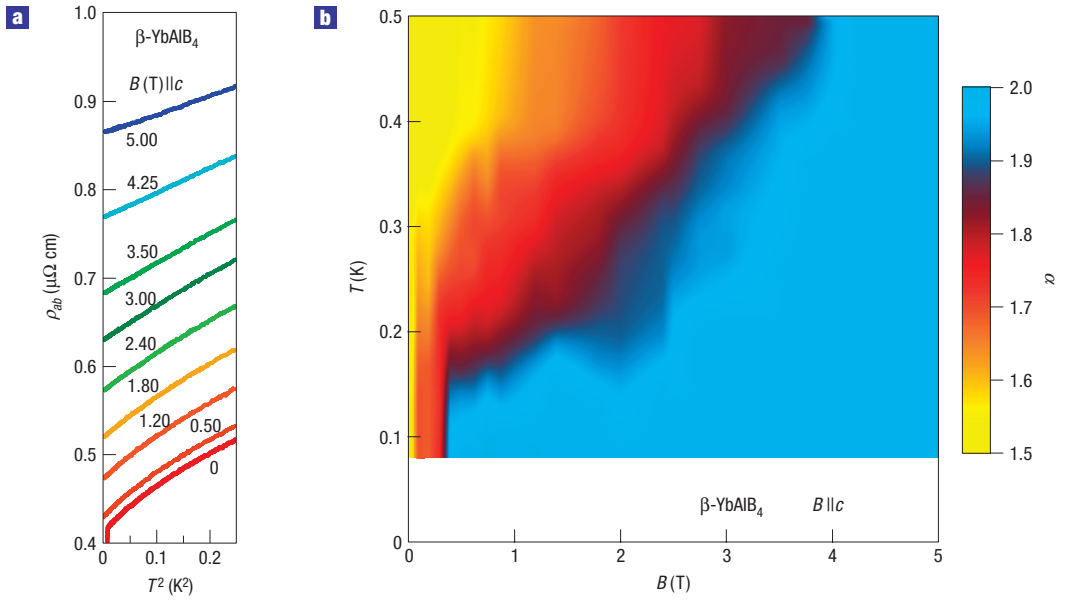

Figure 2 Crossover from non-FL to FL behaviour in the resistivity. a, ab-plane resistivity ρ_{ab} versus T^2 at various magnetic fields along the c axis. **b**, Contour plot of the resistivity exponent α defined by $\Delta\rho = (\rho(T) - \rho(0)) \sim T^{\alpha}$ in the temperature–field phase diagram.

5–6, which is characteristic of a system with strong magnetic correlations. At the low-T limit, A shows a diverging behaviour as B vanishes, following the form $B^{-1/2}$ in the critical regime below ~4 T (Fig. 3d).

Thus, all our observations indicate that as the magnetic field decreases to zero the FL state becomes unstable and A, χ_c and C_M/T all become singular at low T. This is the behaviour expected of a system with a zero-field quantum critical point (QCP), characterized by divergences of A, χ_c and C_M/T of the form T^{-x}, where x is $1/2, 1/3$ and 0^+, respectively (0^+ stands for logarithmic divergence).

We now return to the observation of superconductivity, which emerges at very low temperatures from the non-FL state in samples with residual resistivity ratio RRR > 100. Figure 4a shows the in-plane resistivity of two out of a dozen samples studied, one normal and one superconducting, with RRR of 70 and 300, respectively. Figure 4b shows d.c. magnetization of a sample consisting of a dozen crystals with an average RRR ~ 240 and

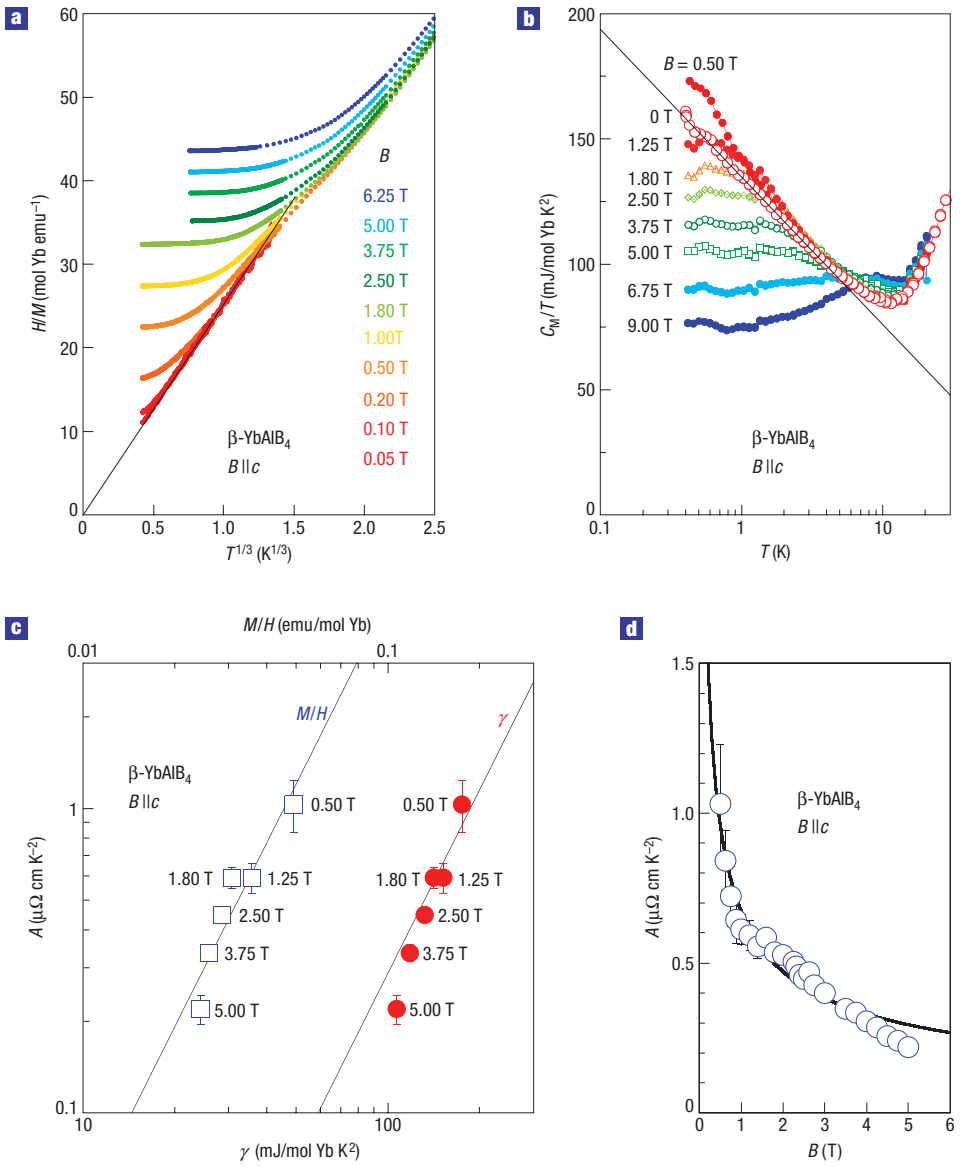

Figure 3 Crossover from non-FL to FL behaviours in the susceptibility and heat capacity. a, Inverse susceptibility H/M versus $T^{1/3}$ at various magnetic fields applied along the c axis. The linear fit indicates a $T^{-1/3}$ dependence for the susceptibility. **b**, Magnetic part of the specific heat divided by temperature, C_M/T, versus the logarithm of the temperature. Here, C_M is obtained by subtracting the specific heat C_P of β-LuAlB$_4$ from that for β-YbAlB$_4$. The linear fit indicates a $\ln(T^*/T)$ dependence with $T^* \sim 200$ K. Above 10 K, C_M/T shows the tail of a Schottky peak due to the crystal-electric-field splitting Δ to the first excited state. Because the peak should be located at $T > 30$ K, Δ must be more than 60 K and must be the origin of the change in slope observed around 40 K in $\chi_c(T)$ and $\rho_{ab}(T)$ in Fig. 1. In keeping with the large temperature scale $T^* \sim 200$ K, the entropy obtained through integration of C_M/T from 0.4 to 30 K reaches only 50% of $R\ln 2$. **c**, Log–log plots of A versus γ and A versus χ for various fields, where $\chi = M/H$. The solid lines represent $A/\gamma^2 \sim 3 \times 10^{-5}\ \mu\Omega\ \mathrm{cm\,K^{-2}(mol\,K^2\,mJ^{-1})^2}$ and $A/\chi^2 \sim 5 \times 10^2\ \mu\Omega\ \mathrm{cm\,K^{-2}\ (mol\ emu^{-1})^2}$. **d**, Field dependence of A. The solid line represents the best fit to the form $B^{-\beta}$, which yields $\beta = 0.50(2)$.

$T_c \sim 68$ mK. The samples are thin plates with the c-axis normal to the plate surface, typically 1 mm across and 0.01 mm thick. Significant shielding of the applied field is evident in both the zero-field-cooled (ZFC) and field-cooled (FC) data. The fraction of the sample volume undergoing a superconducting transition has been estimated by comparing the measurements in β-YbAlB$_4$ with those of Al plates of similar geometry and dimensions. At the lowest temperature of 25 mK we find that the superconducting volume fractions, f, in percentage terms are as follows: for a field in the ab plane $f_{ab} = 15\%$ (ZFC), 6% (FC), and for a field along the c axis $f_c = 45\%$ (ZFC), 5% (FC). These fractions are large enough, given the strong sensitivity of superconductivity to sample purity and probable variation in purity over a typical sample, to indicate that the superconductivity is essentially a bulk phenomenon.

We now turn to a qualitative discussion of our experimental findings, starting with the non-FL normal state and the crossover to an FL state with applied magnetic field. The emergence of non-FL behaviour in heavy-fermion systems has been discussed in terms of the itinerant-electron and localized-electron models[10–14]. In the itinerant-electron model the conduction and f electrons hybridize to form a coherent state characterized by heavy quasiparticles on a Fermi surface enclosing conduction and f-electron states. In

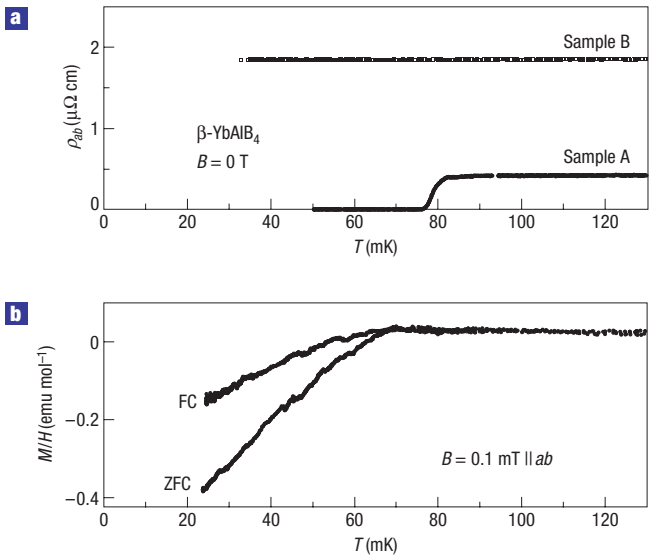

Figure 4 Superconductivity in high-purity single crystals of β-YbAlB$_4$. **a**, Temperature dependence of the low-temperature in-plane resistivity $\rho_{ab}(T)$ for the higher-quality sample A with RRR ~ 300 and for the lower-quality sample B with RRR ~ 70. Only the higher-quality sample A shows superconductivity. **b**, Temperature dependence of the FC and ZFC data of the d.c. susceptibility M/H in a field of 0.1 mT along the *ab* plane for a dozen thin platelike crystals with RRR > 200 and an average RRR ~ 240. By measuring the superconducting shielding effect of Al plates with similar geometry and size, the volume fraction of superconductivity at 25 mK is estimated to be 15 % (ZFC) for the field along the *ab* plane. The reduction of the volume fraction from 100% is probably because the sample thickness along the *c* axis (~10 μm) is of the same order as the penetration depth λ_c along the *c* axis; λ_c is estimated to be ~6 μm by our preliminary experiments to measure the superconducting critical fields.

this model non-FL behaviour and superconductivity can arise, for example, when the system is tuned by some control parameter (doping, pressure or magnetic field) to the border of long-range magnetic order. When the magnetic transition as a function of the 'quantum' tuning parameter is continuous, we have a QCP characterized by a set of non-FL exponents for A, χ_c and C_M/T. In the localized-electron model it is supposed that the coherence between the conduction and f-electron states fails to form completely or otherwise is different from that of the itinerant-electron model. In this model, too, we arrive at non-FL behaviour at a QCP characterized by a set of non-FL exponents.

In both the itinerant- and localized-electron models the non-FL exponents can depend sensitively on a number of details such as the effective dimensionality and nature of the magnetic correlations. We find that the three exponents characterizing A, χ_c and C_M/T in β-YbAlB$_4$ (namely, $x = 1/2, 1/3$ and 0^+, respectively) cannot be understood in a consistent way in terms of either the itinerant- or localized-electron models in their present forms. As an example, we consider the predictions of the itinerant-electron model for three dimensions on the border of antiferromagnetism[10,11]. In the presence of residual disorder this model predicts $x = 1/2$, 0 and 0 for A, χ and C/T, respectively, in only partial agreement with our results for β-YbAlB$_4$ ($x = 1/2, 1/3$ and 0^+). In the same model, but on the border of ferromagnetism, we expect $x = 1/3, 4/3$ and 0^+ for A, χ and C/T, respectively, which is again in only partial agreement with our results for β-YbAlB$_4$.

Systems in which the itinerant-electron model may be applicable are discussed, for example, in refs 1,2,4. Systems in which the localized-electron model is thought to be more appropriate are discussed in refs 15,16 for Au-doped $CeCu_6$ and in refs 6,17–19 for $YbRh_2Si_2$. Here we compare our findings in β-YbAlB$_4$ to those in the latter ytterbium compound. The quantum critical exponents characterizing these two ytterbium materials are different. However, in other respects we find compelling similarities. In both $YbRh_2Si_2$ and β-YbAlB$_4$ the Wilson ratios R_W are high and R_W, A/χ^2 and A/γ^2 are weakly magnetic field dependent in the quantum critical regime. The high value of the Wilson ratio and the weak field dependence of A/χ^2 have been interpreted to suggest that there is a softening of both ferromagnetic as well as antiferromagnetic spin fluctuations[18,19]. We also comment that the crossover temperatures T_0 and T^* are about one order of magnitude higher in β-YbAlB$_4$ than in $YbRh_2Si_2$ (refs 17,18). This suggests that β-YbAlB$_4$ provides a wider accessible T range to identify the asymptotic non-FL exponents and has a more accessible electron-pairing energy scale than in $YbRh_2Si_2$.

Remarkably, we observe a non-FL state in β-YbAlB$_4$ without chemical doping, in zero applied magnetic field and at ambient pressure, a rare example of quantum criticality emerging without external 'quantum' tuning. Furthermore, as in cerium-based compounds close to a QCP (refs 1–6), the superconductivity appears precisely in the non-FL region of the phase diagram where spin fluctuations are expected to be the strongest, suggesting that the pairing mechanism in β-YbAlB$_4$, the first Yb-based heavy-fermion superconductor, is based on magnetic interactions.

The extraordinarily high sensitivity of superconductivity to sample purity in β-YbAlB$_4$ is also consistent with the idea that the Cooper pair state in this system is of an unconventional, non-*s*-wave, character. Superconductivity tends to be suppressed when the electronic mean free path falls below the superconducting coherence length. The latter can be quite short in some cases, such as in the high-temperature superconductors, but long (~50 nm) in a system such as β-YbAlB$_4$ with a very low T_c.

Heavy-fermion superconductivity might be more fragile in the ytterbium than in the corresponding cerium systems because the relevant intersite spin–spin interaction in the former tends to be weaker than in the latter, reducing the superconducting transition temperature while increasing the sensitivity of anisotropic pairing to disorder. Superconductivity in the cerium compounds has been variously described in terms of intersite spin–spin interactions as well as in some cases in terms of effects that arise on the border of density or valence instabilities[1,4,20]. How such effects play out and are relevant in the ytterbium-based systems are questions that we can now begin to address.

METHODS

Single crystals were grown by using the Al-flux method as described in the literature[7]. The excess Al flux was etched by a water solution of sodium hydroxide. To remove any possible impurities attached to the surface during the etching process, single crystals were washed with dilute nitric acid before measurements. X-ray powder diffraction patterns show single-phase samples. Inductively coupled plasma analysis confirms stoichiometry of the compound. Single crystallinity was confirmed by transmission electron microscopy and by single-crystal four-axis X-ray diffraction[7]. Magnetization M above 1.8 K was measured with a commercial superconducting quantum interference device magnetometer whereas M between 0.08 and 2.5 K and under fields up to 7 T was measured by the Faraday method in a dilution refrigerator[21]. To detect the Meissner effect, magnetization measurements were made at 0.1 mT using a superconducting quantum interference device magnetometer in a dilution refrigerator, and a Nb superconducting shield covered with a μ-metal tube was used to eliminate the Earth's magnetic field. Four-terminal resistivity measurements were made by using an a.c. method down to 25 mK. Specific heat C_P was measured by a thermal relaxation method down to 0.4 K.

Received 23 March 2008; accepted 27 May 2008; published 29 June 2008.

References

1. Monthoux, P., Pines, D. & Lonzarich, G. G. Superconductivity without phonons. *Nature* **450**, 1177–1183 (2007).
2. Mathur, N. D. *et al.* Magnetically mediated superconductivity in heavy fermion compounds. *Nature* **394**, 39–43 (1998).
3. Stewart, G. R. Non-Fermi-liquid behaviour in d- and f-electron metals. *Rev. Mod. Phys.* **73**, 797–855 (2001).
4. Yuan, H. Q. *et al.* Observation of two distinct superconducting phases in $CeCu_2Si_2$. *Science* **302**, 2104–2107 (2003).
5. Löhneysen, H. v., Rosch, A., Vojta, M. & Wölfle, P. Fermi-liquid instabilities at magnetic quantum phase transitions. *Rev. Mod. Phys.* **79**, 1015–1075 (2007).
6. Gegenwart, P., Si, Q. & Steglich, F. Quantum criticality in heavy-fermion metals. *Nature Phys.* **4**, 186–197 (2008).
7. Macaluso, R. T. *et al.* Crystal structure and physical properties of polymorphs of $LnAlB_4$ (Ln = Yb, Lu). *Chem. Mater.* **19**, 1918–1922 (2007).
8. Fisk, Z., Yang, K. N., Maple, M. B. & Ott, H. R. in *Valence Fluctuations in Solids* (eds Falicov, L. M., Hanke, W. & Maple, M. B.) 345–347 (North-Holland, New York, 1981).
9. Kadowaki, K. & Woods, S. B. Universal relationship of the resistivity and specific heat in heavy-Fermion compounds. *Solid State Commun.* **58**, 507–509 (1986).
10. Moriya, T. *Spin Fluctuations in Itinerant Electron Magnetism* (Springer, Berlin, 1985).
11. Millis, A. J. Effect of a nonzero temperature on quantum critical points in itinerant fermion systems. *Phys. Rev. B* **48**, 7183–7196 (1993).
12. Coleman, P., Pépin, C., Si, Q. & Ramazashvili, R. How do Fermi liquids get heavy and die? *J. Phys. Condens. Matter* **13**, R723–R738 (2001).
13. Si, Q., Rabello, S., Ingersent, K. & Smith, J. L. Locally critical quantum phase transitions in strongly correlated metals. *Nature* **413**, 804–808 (2001).
14. Senthil, T., Sachdev, S. & Vojta, M. Fractionalized Fermi liquids. *Phys. Rev. Lett.* **90**, 216403 (2003).
15. Löhneysen, H. v. *et al.* Non-Fermi-liquid behaviour in a heavy-fermion alloy at a magnetic instability. *Phys. Rev. Lett.* **72**, 3262–3265 (1994).
16. Schröder, A. *et al.* Onset of antiferromagnetism in heavy-fermion metals. *Nature* **407**, 351–355 (2000).
17. Trovarelli, O. *et al.* $YbRh_2Si_2$: Pronounced non-Fermi-liquid effects above a low-lying magnetic phase transition. *Phys. Rev. Lett.* **85**, 626–629 (2000).
18. Custers, J. *et al.* The break-up of heavy electrons at a quantum critical point. *Nature* **424**, 524–527 (2003).
19. Gegenwart, P. *et al.* Multiple energy scales at a quantum critical point. *Science* **315**, 969–971 (2007).
20. Holmes, A. T., Jaccard, D. & Miyake, K. Signatures of valence fluctuations in $CeCu_2Si_2$ under high pressure. *Phys. Rev. B* **69**, 024508 (2004).
21. Sakakibara, T., Mitamura, H., Tayama, T. & Amitsuka, H. Faraday force magnetometer for high-sensitivity magnetization measurements at very low temperatures and high fields. *Japan. J. Appl. Phys.* **33**, 5067–5072 (1994).

Acknowledgements

We thank M. Ichihara and Y. Kiuchi for their transmission electron microscopy and inductively coupled plasma analyses, and A. Kusmartseva, S. S. Saxena, Y. Matsumoto, T. Tomita, J. Yamaura, Y. Uwatoko, D. Pines, Julia Y. Chan, M. Surtherland, E. O'Farrell, Q. Si, M. Imada and C. Pépin for discussions. This work has been supported in part by Grants-in-Aid for Scientific Research from JSPS, by a Grant-in-Aid for Scientific Research on Priority Areas as well as the 21COE program 'Diversity and Universality in Physics' from MEXT of Japan and by the NSF of the United States through DMR-0710492.

Author information

Reprints and permission information is available online at http://npg.nature.com/reprintsandpermissions. Correspondence and requests for materials should be addressed to S.N.